

The Real-Gas Effect in Single-bubble Sonoluminescence ⁶

Li YUAN*, Wei WEI**, Cunyan HO[†], Mingchung CHU[†] and Puitang LEUNG[†]

* (LSEC, Institute of Computational Mathematics and Scientific-Engineering Computing, Chinese Academy of Sciences, Beijing 100080, China)

** (Center for Nonlinear Sciences, University of Science and Technology of China, Hefei 230026, China)

[†] (Department of Physics, The Chinese University of Hong Kong, Shatin, Hong Kong, China)

E-mail: lyuan@lsec.cc.ac.cn

Abstract: The full set of hydrodynamic equations governing the oscillation of a bubble is solved numerically by using a modified equation of state with ionization. We show that the hydro-thermal process in the form of compression waves and low-level ionization are dominant inside a sonoluminescing bubble for a wide range of driving pressure. The resulting thermal bremsstrahlung radiation has pulse heights and widths that agree with experimental data for cases considered in this paper.

Keywords: single-bubble sonoluminescence, ionization, bremsstrahlung

Introduction

The remarkable discovery that acoustic energy can be converted to light through an oscillating air bubble in water has triggered wide-spread studies in single-bubble sonoluminescence (SBSL) ^[1]. Under certain conditions, a narrow and regular flash of light with a width of about 50-250 ps is emitted in each cycle of the bubble oscillation^[2]. A number of models were proposed to explain the cause of light emission, such as thermal black-body radiation^[3], thermal bremsstrahlung^[4], collision-induced emission^[5], and quantum-vacuum radiation^[6]. The suitability of a model relies on how real the hydro-thermal process inside the bubble is described. Previous calculations based on inviscid spherical hydrodynamics suggested that a converging shock produced high temperature and pressure and the reflected diverging shock quenched them in picosecond time scale^[3,4,7-9]. More recent studies^[10-13] that include diffusive transport neglected elsewhere demonstrate that the shock wave is not essential for stable sonoluminescence which is mainly argon SBSL according to the argon-rectification hypothesis^[14]. Rather, a smooth compression wave emerges naturally in a collapsing bubble. Nevertheless, the predicted temperature is on the order of several 10^4 K and can produce ionization, thus resulting in the above-mentioned thermal light emission. A major goal in this paper is to study the effects of ionization occurred at such high temperature conditions and its relevance to SBSL.

1 Governing Equations and Numerical Method

Neglecting the mass exchange between the bubble and the surrounding water, the dynamics of a spherically oscillating bubble is described by the compressible Navier-Stokes equations

$$\frac{\partial \mathbf{Q}}{\partial t} + \frac{\partial \mathbf{F}(\mathbf{Q})}{\partial x} = \mathbf{S}(\mathbf{Q}) + \mathbf{S}_v(\mathbf{Q}) + \mathbf{S}_s(\mathbf{Q}) \quad (1)$$

⁶The paper was received on Apr.9, 1999

where $x \equiv r/R(t)$ has been used to transform the equations from 1-D spherical coordinate $r \in [0, R]$ to a fixed domain $x \in [0, 1]$. Here $\mathbf{Q} = R(\rho\mathbf{f}, \rho, \rho v, \rho E)^T$, with $E = e + \frac{1}{2}v^2$ the total energy per mass, $R, \mathbf{f}, \rho, v, P, T$, and e the bubble radius, mass fraction vector, density, radial velocity, pressure, temperature, and internal energy per unit mass respectively. The inviscid fluxes are $\mathbf{F} = [\rho(v-x\dot{R})\mathbf{f}, \rho(v-x\dot{R}), \rho v^2 + P - \rho v x \dot{R}, (\rho E + P)v - \rho E x \dot{R}]^T$, and the spherical sources are $\mathbf{S} = -2v[\rho\mathbf{f}, \rho, \rho v, (\rho E + P)]^T/x$. The diffusive transport terms are given by $\mathbf{S}_v = \{\partial_x(x^2 \frac{\rho D}{R} \partial_x \mathbf{f}), \partial_x(x^2 \tau_{rr}) + x\tau_{rr}, \partial_x[x^2(v\tau_{rr} + k\partial_x T/R + \frac{\rho D}{R} \sum_{i=1}^{N_s} h_i \partial_x f_i)]\}^T/x^2$, where $\tau_{rr} = 4\mu(\partial_x v - v/x)/3R$ is the normal viscous stress, k is the coefficient of thermal conductivity, h_i is the thermal enthalpy of species i , N_s is the total number of species including atm, ions and electrons. μ is the dynamic viscosity, and D the binary diffusion coefficient of species.

The hydrodynamics of the bubble is affected by the compressibility of the gas. We consider an argon bubble. We modify a recently used EOS of argon in [13] by taking into account the non-equilibrium ionization process. The EOS is constructed so that pressure P and internal energy e can be decomposed into three parts:

$$\begin{aligned} P(\rho, T, \mathbf{f}) &= P_c(\rho) + P_n(\rho, T, \mathbf{f}) + p_e(\rho, T, \mathbf{f}) \\ e(\rho, T, \mathbf{f}) &= e_c(\rho) + e_n(\rho, T, \mathbf{f}) + e_e(\rho, T, \mathbf{f}) \end{aligned} \quad (2)$$

The first cold curve part is exactly the same as that in [13] which we do not repeat here. The nuclear motion part includes the ideal gas contribution and a configurational soft-sphere piece which represents the nonideal behavior of the dense fluid,

$$\begin{aligned} P_n(\rho, T, \mathbf{f}) &= \left(\sum_{i=0}^L \frac{f_i}{m_i} \right) k\rho T + \frac{1}{18} \left(\sum_{i=0}^L \frac{f_i}{m_i} \right) k\rho T q j (j+4) \eta^{j/9} \tau^{1/3} \\ e_n(\rho, T, \mathbf{f}) &= \frac{3}{2} \left(\sum_{i=0}^L \frac{f_i}{m_i} \right) kT + \frac{1}{6} \left(\sum_{i=0}^L \frac{f_i}{m_i} \right) kT q (j+4) \eta^{j/9} \tau^{1/3} \end{aligned} \quad (3)$$

Here $\mathbf{f} = (f_0, \dots, f_L)$ is the mass fraction vector, L is the the upper critical level of ionization considered here, m_i is the mass of an atom ($i=0$) or an ion with a charge i . $k = 1.3805 \times 10^{-23}$ J/K is the Boltzmann constant, $\tau = T_1/T$, where T_1 is a reference temperature set to 0.001 Kev. $\eta = \rho/\rho_0$, where ρ_0 is the density of the cold solid at $P=0$. The parameters q and j are available to fit high-temperature experimental EOS data. We use $q=0.2$ and $j=6$.

The electrons are treated as ideal gas particles so that the electron pressure and energy are

$$\begin{aligned} P_e &= \frac{f_e}{m_e} k\rho T \\ e_e &= \frac{3}{2} kT + k \sum_{i=1}^L \sum_{j=i}^L \left(\frac{f_j}{m_j} \right) T_i \end{aligned} \quad (4)$$

where m_e is the mass of an electron and the mass fraction of electron f_e is determined by using the law of conservation of species: $f_e = 1 - \sum_{i=0}^L f_i$. The second term in the right-hand side of e_e represents the energy required for ionization. The ionization level L is set to 5 on which the ionization potential are far above the present temperature range.

The process of electron collisional ionization, radiative recombination and three-body recombination is considered in the same way as [15].

The Navier-Stokes equations are coupled to the Rayleigh-Plesset (RP) equation that describes the bubble wall motion. We chose a more complete RP equation^[16] that includes

correction terms to first order in the bubble-wall Mach number M and allows for a variable speed of sound in the liquid c_l

$$\frac{1-M}{1+M}R\ddot{R} + \frac{3-M}{2(1+M)}\dot{R}^2 = H_b - \frac{P_s(t')}{\rho_\infty} + \frac{t_R\dot{H}_b}{1+M} \quad (5)$$

Here overdots denote time derivatives, $t_R \equiv R/c_l$, $t' \equiv t + t_R$, ρ_∞ is the ambient density, $P_s(t') = -P_a \sin(\omega t')$ the pressure of the sound field with frequency ω and amplitude P_a , and H_b is the enthalpy of the liquid. c_l and H_b are obtained using an EOS of water in the modified Tait form^[17].

To take into account the heat transfer between the bubble and the surrounding water, we also solve the following energy equation for the water^[10].

$$\frac{\partial T_l}{\partial t} + v_l \frac{\partial T_l}{\partial r} = D_l \frac{1}{r^2} \frac{\partial}{\partial r} \left(r^2 \frac{\partial T_l}{\partial r} \right) \quad (6)$$

where T_l , v_l and D_l are the temperature, velocity and thermal diffusion coefficient of the liquid.

An bremsstrahlung radiation power is computed by

$$P_{br} = 1.57 \times 10^{-40} \sum_{i=1}^L i^2 n_i^2 T^{1/2} \quad [w/m^3] \quad (7)$$

where $n_i = f_i \rho / m_i$ is number density.

We apply a second-order TVD scheme^[18] to the convective terms. 400 grid points are used for the N-S solution in the bubble and 80 points for the water temperature equation the liquid. We calculate the bubble oscillation starting from an ambient radius R_0 by using the RP equation with isothermal polytropic index. The RP solution is terminated at $3R_0$ of the main collapse, which serves as a good initial flow field. From this point onward, we switch to the solution of the full hydrodynamics. The initial number density, hence the mass fraction of ions and electrons are estimated by using the Saha equation.

2 Computational Results

We consider the ambius $P_0 = 1$ atm, $T_0 = 300$ K, the driving pressure has a frequency $\omega/2\pi = 26.4$ kHz, and other parameters are set to standard values. Whereas R_0 depends on the driving pressure in nature, we chose R_0 to be $4.5 \mu\text{m}$ located in the stable range of SBSL. We computed several cases in which P_a varies from 1.275 atm to 1.45 atm, approximately spanning the range of stable SBSL.

For driving pressures between 1.275 atm and 1.45 atm, the computed bremsstrahlung power falls nicely into experimental ranges, both in the magnitude and in the time width of the light flash. We show in Fig.2 the total radiation power. We note that the duration is generally longer that those from a shock wave model, but in better agreement with recent experiments.

The spatial profiles of temperature and velocity are compared between the present EOS with ionization and the original EOS (YEOS) without ionization as shown in Fig.2. From the velocity profile we can see that a steep compressional wave is formed if ionization is considered, while more gentle compression wave appears in YEOS. This shows that ionization tends to enhance the violence of the hydrodynamic process. The temperature profile in the former case clearly shows an ionized zone with lower temperature in the inner part of the bubble. We can also see that the ionized zone is quite wide and only Ar^+ is the dominant ion, in sharp contrast to the thin layer and multiple ionizations of earlier works^[15].

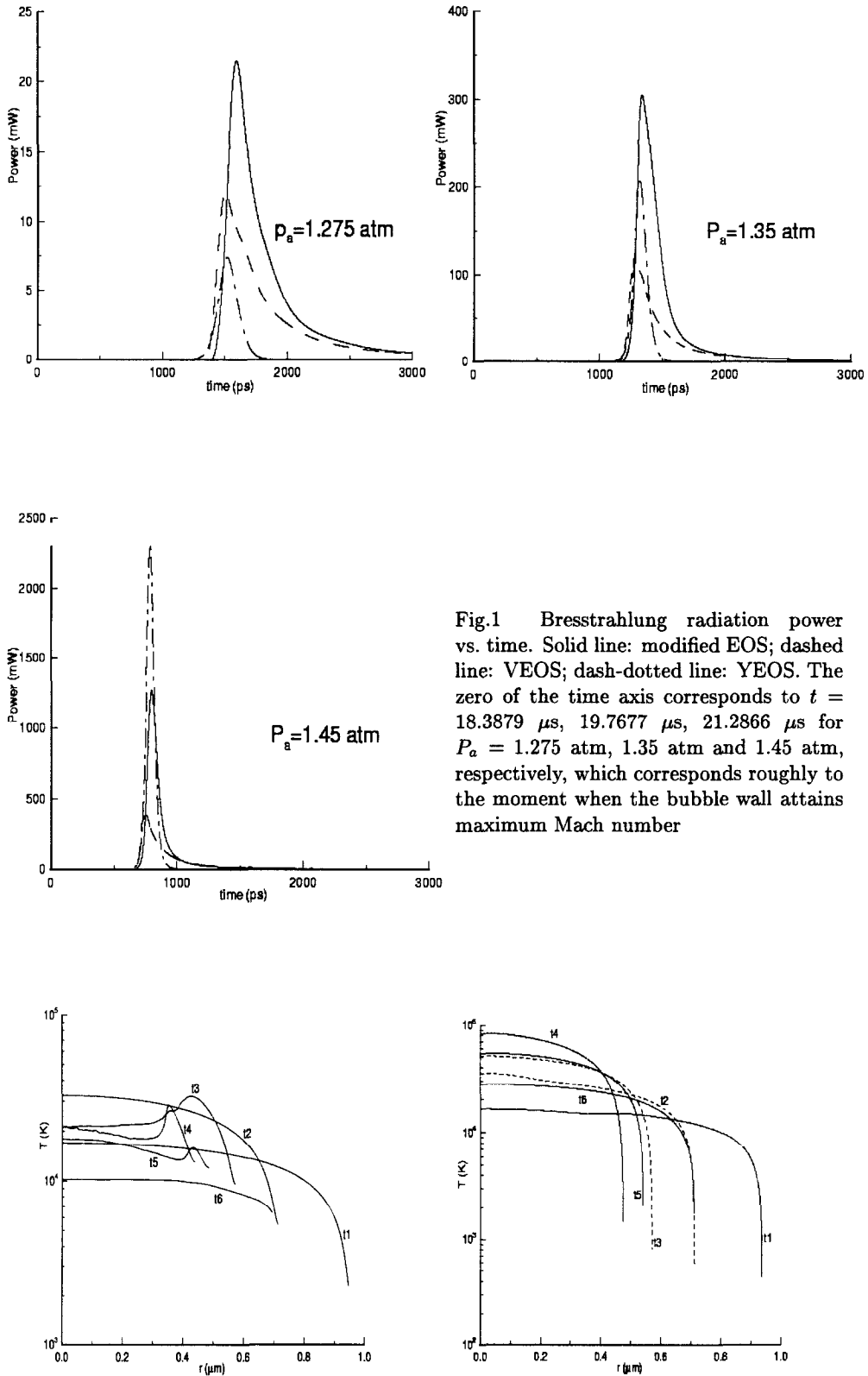


Fig.1 Bremsstrahlung radiation power vs. time. Solid line: modified EOS; dashed line: VEOS; dash-dotted line: YEOS. The zero of the time axis corresponds to $t = 18.3879 \mu\text{s}, 19.7677 \mu\text{s}, 21.2866 \mu\text{s}$ for $P_a = 1.275$ atm, 1.35 atm and 1.45 atm, respectively, which corresponds roughly to the moment when the bubble wall attains maximum Mach number

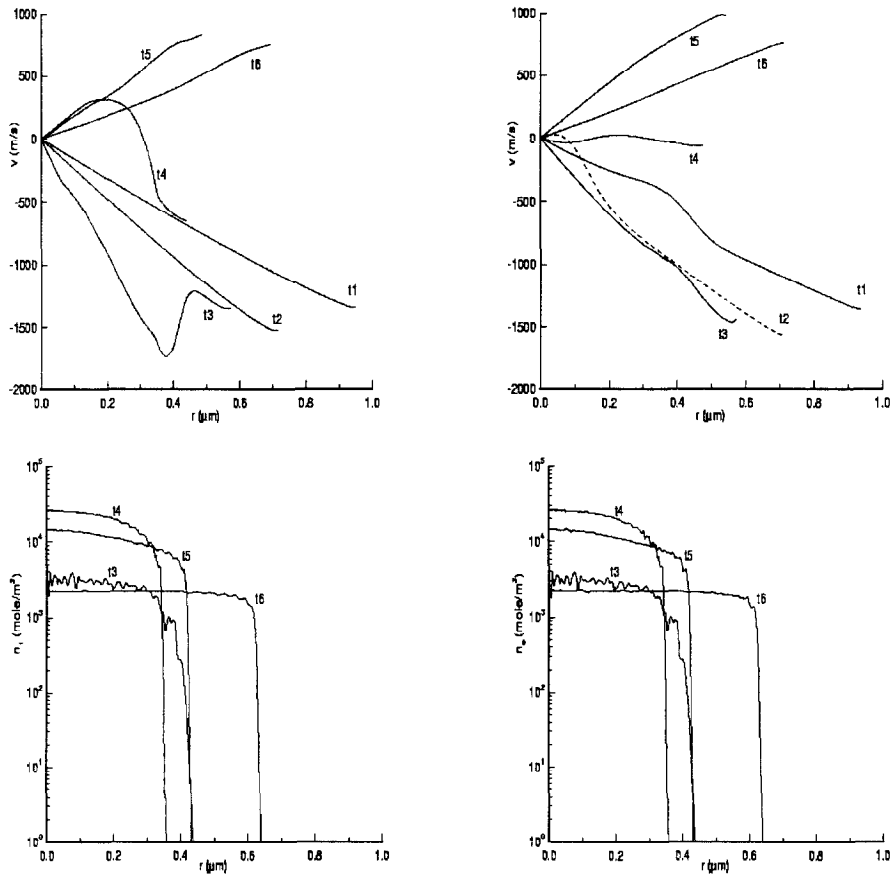


Fig.2 The snapshots of the profiles of the temperature and velocity, and the number density of electron and Ar^+ for $P_a = 1.35$ atm. $t_1 = -409$ ps, $t_2 = -246$ ps, $t_3 = -148$, $t_4 = -30$ ps, $t_5 = 96$ ps, $t_6 = 334$ ps. The reference time $t_{R\min} = 19.769072 \mu\text{s}$

3 Conclusion

In conclusion, based on the numerical simulation of a more realistic model, we have shown that the hydro-thermal process with compression waves are strong enough to make the gas partially ionized. The ionized zone is wide instead of narrow. The ionization enhances the steepening of the compression wave. Although the first-level ionization dominates, the resulting thermal bremsstrahlung radiation has pulse heights and widths that agree with experimental data for cases considered here.

References

- [1] Gaitan, D. F., et al., J. Acoust. Soc. Am., 1992, 91: 3166; Barber, B. P., et al., Phys. Rep., 1997, 281: 65, and references therein
- [2] Gompf, B., et al., Phys. Rev. Lett., 1997, 79: 1405
- [3] Moss, W., et al., Phys. Fluids, 1994, 6(9): 2979
- [4] Wu, C. C. and Roberts, P. H., Phys. Rev. Lett., 1993, 70: 3424
- [5] Frommhold, L. and Atchley, A. A., Phys. Rev. Lett., 1994, 73: 2883; Phys. Rev., 1998, E58: 1899
- [6] Eberlein, C. E., Phys. Rev. Lett., 1996, 76: 3842

- [7] Kondić, L., Gersten, J. I. and Yuan, C., Phys. Rev., 1995, E52: 4976
- [8] Chu, M. -C. and Leung, D., J. Phys. Cond. Matt., 1997, 9: 3387
- [9] Moss, W., et al., Science, 1997, 276: 1398
- [10] Vuong, V. Q. and Szeri, A. J., Phys. Fluids, 1996, 8: 2354
- [11] Yuan, L., et al., Phys. Rev., 1998, E57: 4265
- [12] Cheng, H. Y., Chu, M. C., Leung, P. T. and Yuan, L., Phys. Rev., 1998, E58: R2705
- [13] Vuong, V. Q., Szeri, A. J. and Young, D. A., Phys. Fluids, 1999, 11: 10
- [14] Lohse, D., et al., Phys. Rev. Lett., 1997, 78: 1359
- [15] Xu, N., Wang, L. and Hu, X. W., Phys. Rev., 1998, E57: 1615
- [16] Kamath, V. and Prosperetti, A., J. Acoust. Soc. Am., 1989, 85: 1538
- [17] Prosperetti, A. and Lezzi, A., J. Fluid Mech., 1996, 168: 457
- [18] Yee, H. C., A class of high-resolution explicit and implicit shock-capturing methods, NASA TM 101088, 1989

The Absolute and Convective Secondary Instabilities in the Conduction Regime ⁷

Jianjun TAO and Dachun YAN

(Dept. of Mechanics & Engineering Sciences, Peking University, Beijing 100871, China)

Abstract: Convective and absolute instabilities in the conduction regime of a vertical heated slot are investigated. It is found that in a large range of Prandtl number ($0 < Pr < 2000$) different instability mode has different characteristics: the stationary mode is absolute instability while the traveling wave mode is convective instability. When $Pr > 12$, a secondary instability appears with stationary mode, and it is proven that even at large Prandtl numbers the stationary mode still exists.

Keywords: absolute instability, convective instability, conduction regime

Introduction

Generally, a velocity profile is called absolutely unstable if localized disturbances can spread upstream and downstream and contaminate the entire flow eventually; by contrast, the profile will be called convectively unstable if the disturbance are swept away from the source. The absolute instability was found downstream in the convection boundary layer when the heated vertical plate was immersed in a thermally stratified medium^[1]. In closed flows, such as Rayleigh-Bernard convection or Taylor-Coutte flow, because of the reflection symmetry, the critical Reynolds numbers of convective and absolute instability coincide. Recently, the primary advances in closed flows centered on the study of binary fluid mixtures with heated bottom^[2]. But for another important case, the vertical heated slot with large ratio of height and width, how its convective or absolute instability evolves has not been studied.

The convection flow in the vertical slot heated on both sides has many distinct characteristics that make it different from other closed flows. At low Grashof number or with high ratio of height to width, heat is transferred across the slot primarily by conduction. The instability of the conduction regime was studied analytically and experimentally^[3,4], and two unstable modes were found in the first stage of transition to turbulence: stationary convection rolls at low Prandtl number and traveling waves at high Prandtl number. Since

⁷The paper was received on Mar.20, 1999